Published in final edited form as:
Dev Biol. 2011 November 1; 359(1): 47–58. doi:10.1016/j.ydbio.2011.08.014.

The gap junctional protein INX-14 functions in oocyte precursors to promote *C. elegans* sperm guidance

Johnathan W. Edmonds[1], **Shauna L. McKinney**[2], **Jeevan K. Prasain**[3], and **Michael A. Miller**[1,*]

[1]Department of Cell Biology, University of Alabama at Birmingham, Birmingham, Alabama 35294, USA

[2]Division of Reproductive Endocrinology and Infertility, Department of Obstetrics and Gynecology, University of Alabama at Birmingham, Birmingham, AL 35294, USA

[3]Department of Pharmacology and Toxicology, University of Alabama at Birmingham, Birmingham, Alabama 35294, USA

Abstract

Innexins are the subunits of invertebrate gap junctions. Here we show that the innexin INX-14 promotes sperm guidance to the fertilization site in the *C. elegans* hermaphrodite reproductive tract. *inx-14* loss causes cell nonautonomous defects in sperm migration velocity and directional velocity. Results from genetic and immunocytochemical analyses provide strong evidence that INX-14 acts in transcriptionally active oocyte precursors in the distal gonad, not in transcriptionally inactive oocytes that synthesize prostaglandin sperm-attracting cues. Somatic gonadal sheath cell interaction is necessary for INX-14 function, likely via INX-8 and INX-9 expressed in sheath cells. However, electron microscopy has not identified gap junctions in oocyte precursors, suggesting that INX-14 acts in a channel-independent manner or INX-14 channels are difficult to document. INX-14 promotes prostaglandin signaling to sperm at a step after F-series prostaglandin synthesis in oocytes. Taken together, our results support the model that INX-14 functions in a somatic gonad/germ cell signaling mechanism essential for sperm function. We propose that this mechanism regulates the transcription of a factor(s) that modulates prostaglandin metabolism, transport, or activity in the reproductive tract.

Keywords

innexin; pannexin; gap junction; prostaglandin; *C. elegans*; fertilization; sperm; oocyte; FOXO; chemotaxis

Introduction

Gap junctions are channels between adjacent cells that facilitate passage of small molecules, such as cAMP and inositol triphosphate (Harris, 2001; Nicholson, 2003; Phelan and Starich, 2001). The basic protein subunits of gap junctions belong to two families called connexins and pannexins (Goodenough, 1974; Mroue et al., 2011; Panchin, 2005). These subunits form

*Corresponding author: Michael A. Miller (mamiller@uab.edu).

hexameric rings at the cell surface known as hemichannels, which connect to hemichannels on adjacent cells to form the channel (Unger et al., 1999). Hemichannels can consist of a single subunit or multiple subunits and connect to hemichannels with identical or different subunit compositions. Gap junctions allow for electrical coupling between cells, as well as for passage of molecules that initiate signal transduction and gene expression (Bevans et al., 1998; Niessen et al., 2000). In addition, channel-independent functions have been proposed (Dbouk et al., 2009). Perhaps the most common examples of gap junctions are those found connecting neurons at electrical synapses. However, gap junctions can have diverse functions in development and disease (Mroue et al., 2011).

In the mammalian ovary, gap junctions between oocytes and surrounding cumulus cells are essential for folliculogenesis and oogenesis (Gershon et al., 2008). At least 5 connexins are expressed in the mouse follicle, although Cx37 and Cx43 are the most abundant and well studied (Kidder and Mhawi, 2002). In Cx37 knockout mice, oocyte development arrests before meiotic competence occurs and mature Graafian follicles are absent (Simon et al., 1997). Cx43 knockout mice die shortly after birth due to heart malformation (Reaume et al., 1995). Transplantation and chimeric studies support the view that Cx43 promotes follicle growth and oocyte meiotic progression (Ackert et al., 2001; Gittens and Kidder, 2005; Juneja et al., 1999). Cx37 appears to function primarily in the oocytes and cumulus cells, whereas Cx43 appears to function in the granulosa cells (Gittens and Kidder, 2005). In addition to follicle development, gap junctions are thought to maintain meiotic arrest in the Graafian follicle (Anderson and Albertini, 1976; Dekel, 2005). The early folliculogenesis defects of Cx37 and Cx43 knockout mice, as well as potential redundancy among connexin genes have complicated efforts to understand all gap junction functions in the mammalian ovary.

We have been using the *C. elegans* gonad as a model to investigate gap junctions in reproduction (Whitten and Miller, 2007). The adult hermaphrodite gonad consists of two U-shaped arms that share a common uterus (Yamamoto et al., 2005). Germ cells proliferate and initiate oocyte differentiation in the distal gonad, whereas oocytes complete differentiation in the proximal gonad. Somatic gonadal sheath cells surround the germ cells and oocytes. Electron microscopy has detected gap junctions between oocytes and sheath cells in the proximal gonad, but not between germ cells and sheath cells in the distal gonad (Hall et al., 1999). Additionally, gap junctions have been found between adjacent sheath cells (Hall et al., 1999; Whitten and Miller, 2007). During oocyte meiotic maturation and ovulation, the most proximal oocyte enters the spermatheca, a sac-like structure where fertilization occurs. Motile amoeboid sperm actively target the spermatheca and compete to fertilize ovulating oocytes (Han et al., 2010). During mating, males inject sperm through the hermaphrodite vulva. Sperm become activated for motility and migrate around fertilized eggs and across uterine walls to the spermatheca.

Invertebrates form gap junctions using pannexin family members called innexins (Baranova et al., 2004; Phelan et al., 1998; Starich et al., 2001). While connexins and innexins differ in sequence, they share structural and functional properties. Both families are characterized by four transmembrane domains with two to three cysteine residues in the extracellular loops. The *C. elegans* genome encodes twenty-five innexins, eleven of which are expressed in the developing or adult reproductive system (Altun et al., 2009; Starich et al., 2001). The innexins INX-14 and INX-22 co-localize at the interface between oocytes and sheath cells in the proximal gonad, where they are thought to form gap junctions (Govindan et al., 2009). Sperm secrete a signaling molecule called MSP (major sperm protein) to induce oocyte meiotic maturation and ovulation (Miller et al., 2001). *inx-14* and *inx-22* are required in the oocytes to maintain meiotic arrest in the absence of sperm and MSP is thought to antagonize this function (Govindan et al., 2006; Whitten and Miller, 2007). Null mutations in *inx-14*

cause germ cell proliferation and differentiation defects, whereas *inx-22* is not essential for fertility (Govindan et al., 2009; Whitten and Miller, 2007). INX-14 and INX-22 also co-localize at the interface between germ cells and sheath cells in the adult distal gonad, but their function(s) here was not known (Govindan et al., 2009).

We have shown that *inx-14* RNAi causes abnormal sperm distribution in the hermaphrodite uterus, raising the possibility that innexins regulate sperm guidance (Whitten and Miller, 2007). Oocytes in the proximal gonad synthesize sperm-attracting F-series prostaglandins from polyunsaturated fatty acid (PUFA) precursors provided in yolk lipoprotein complexes (Edmonds et al., 2010; Kubagawa et al., 2006). Prostaglandin deficiency causes cell nonautonomous defects in sperm migration velocity and directional velocity, resulting in abnormal targeting to the spermatheca. We have shown that microinjecting F-series prostaglandins into the uterus of prostaglandin-deficient hermaphrodites stimulates sperm migration (Edmonds et al., 2010). Here we provide strong evidence that INX-14 functions in transcriptionally active oocyte precursors in the distal gonad to promote sperm guidance. However, *inx-14* promotes prostaglandin function at a step downstream of F-series prostaglandin synthesis in transcriptionally inactive oocytes. Our results support the model that sheath cell/germ cell signaling via innexins regulates the transcription of a factor(s) controlling prostaglandin transport or activity. Hence, interactions between the somatic gonad and oocytes early in oogenesis can influence later processes critical for sperm function.

Results

Nonautonomous control of sperm guidance by INX-14

inx-14 has been shown to function in the germ line to regulate germ cell proliferation, differentiation, oocyte maturation, and sperm distribution within the uterus (Govindan et al., 2006; Govindan et al., 2009; Whitten and Miller, 2007). To investigate the mechanism by which *inx-14* controls sperm distribution, we examined *inx-14(RNAi)* hermaphrodites and *inx-14(ag17)* mutant hermaphrodites. Null mutations in *inx-14* cause germ cell proliferation and differentiation defects that prevent oogenesis. To bypass this developmental requirement, we initiate RNAi during the L4 and adult stages. The *ag17* allele is a hypomorphic missense mutation that results in an arginine to histidine substitution near the end of the third transmembrane domain (Miyata et al., 2008). *inx-14(ag17)* mutants were reported to exhibit a partially penetrant sterility phenotype leading to a smaller brood size at 25°C. We grew *inx-14(ag17)* mutants at 20°C until the L4 or young adult stages and then shifted the mutants to 25°C for 24 to 36 hours. Under these conditions, *inx-14* mutant and RNAi gonads contain well-developed oocytes that progress through meiosis, the events of fertilization, and early embryonic development identical to those of wild-type hermaphrodites. Previous studies have shown that *inx-14(RNAi)* causes precocious oocyte maturation in the absence of sperm (Govindan et al., 2006; Whitten and Miller, 2007). We observed slightly elevated oocyte maturation rates in unmated *inx-14(ag17); fog-2(q71)* females relative to unmated control *fog-2(q71)* females (Fig. S1). The phenotype is less severe than the *inx-14* RNAi phenotype, supporting the hypothesis that the *ag17* mutation causes reduced *inx-14* function. We conclude that *inx-14(RNAi)* and *inx-14(ag17)* mutants can be used to study INX-14 function in adults, independent of its role in germline development.

To investigate the role of INX-14 in sperm guidance, we mated wild-type MitoTracker-labeled (MT) males to adult *inx-14(ag17)* mutant and *inx-14(RNAi)* hermaphrodites. In these experiments, sperm motility within the uterus is measured immediately after mating and sperm distribution is evaluated one hour after mating (Edmonds et al., 2010; Kubagawa et al., 2006). The uterus is divided into three zones for quantification (Fig. 1A). Sperm

migration velocity, directional velocity toward the spermatheca, and reversal frequency are measured in zone 2, the region within the uterus between the vulva and spermatheca. Control matings show that 92% of sperm reach the spermatheca (zone 3) in one hour. In contrast, wild-type sperm fail to accumulate efficiently at the spermatheca of *inx-14(ag17)* mutants one hour after mating (Fig. 1A-C). Time-lapse imaging following mating indicate that wild-type sperm in *inx-14(ag17)* mutant hermaphrodites migrate through the uterus with reduced overall velocity, reduced directional velocity, and increased reversal frequency compared to the control (Table 1, compare line 2 to 1; $P < 0.001$). *inx-14(RNAi)* causes a similar, albeit more severe phenotype than that seen in *inx-14(ag17)* hermaphrodites (Fig. 1C, D and Table 1, lines 1–3). Only 40% of sperm reach the spermatheca of *inx-14(RNAi)* hermaphrodites one hour after mating. Sperm migrate through the uterus with reduced velocity, no directional velocity, and a higher reversal rate compared to the control (Table 1, compare line 3 to 1; $P < 0.001$). *inx-14(RNAi)* sperm motility defects are nearly identical to those observed in prostaglandin-deficient mutants (Edmonds et al., 2010; Kubagawa et al., 2006). These results indicate that *inx-14* is required cell non-autonomously for sperm motility and guidance to the spermatheca.

Govindan et al. (2009) have shown that INX-22 co-localizes with INX-14 in germ cells and oocytes (Govindan et al., 2009). *inx-14* and *inx-22* function together to inhibit oocyte maturation in the absence of sperm (Govindan et al., 2006; Whitten and Miller, 2007). We previously showed that sperm accumulate near the spermatheca of mated *inx-22(tm1661)* null mutants (Whitten and Miller, 2007). To quantify the effects of *inx-22* loss on sperm motility, we measured sperm distribution in mated *inx-22(tm1661)* uteri one hour after mating. Sperm distribution is *inx-22* mutants is not significantly different than distribution in controls (Fig. 1B and E; $P > 0.05$). Furthermore, sperm motility values in the mutants are similar to values in controls (Table 1, compare line 4 to 1). Therefore, *inx-22* is not essential for sperm guidance and the mechanism by which *inx-14* functions in oocyte maturation is different than the mechanism in sperm guidance.

INX-14 acts in the distal gonad to regulate sperm guidance

INX-14 is expressed in germ cells in the distal gonad, as well as in differentiating oocytes in the proximal gonad (Govindan et al., 2009). To further investigate INX-14 localization, we performed immunocytochemistry using a polyclonal antibody against INX-14 (generously provided by T. Starich and D. Greenstein). INX-14 immunostaining of wild-type gonads confirmed the previously reported expression pattern (Fig. 2A, B). INX-14 localizes to discrete puncta at the sheath/oocyte interface in the proximal gonad and the germ cell/sheath interface in the distal gonad (Fig. 2A, B, and K). *inx-14(RNAi)* causes a near complete loss of INX-14 expression in both the proximal and distal gonads (Fig. 2C, D, and K). Next, we examined INX-14 localization in *inx-14(ag17)* animals. We found that the *ag17* mutation preferentially affected INX-14 localization in the distal gonad relative to the proximal gonad (Fig. 2E, F). Quantification shows that INX-14 puncta are reduced in *inx-14(ag17)* proximal gonads relative to wild-type proximal gonads (Fig. 2K; $P < 0.001$). However, INX-14 puncta in *inx-14(ag17)* distal gonads are largely absent. Faint staining was observed in the germ cell cytoplasm, but it was difficult to determine if INX-14 was mislocalized or degraded. These data raise the possibility that INX-14 functions in the distal germ cells to regulate sperm guidance. To further investigate this possibility, we examined $G\alpha_s$-adenylate cyclase pathway genes required for signaling through proximal sheath/oocyte gap junctions (Govindan et al., 2006; Govindan et al., 2009). Inhibition of G_s alpha subunit *gsa-1* (Fig. 3A), G_o alpha subunit *goa-1* (Fig. 3B), or cAMP-dependent protein kinase regulatory subunit *kin-2* (Fig. 3C) function has little effect on sperm guidance, even though sheath contact is essential for INX-14 function in this process (see below). These data argue against INX-14 acting in the proximal gonad.

INX-22 co-localizes with INX-14 in germ cells and oocytes (Govindan et al., 2009), yet *inx-22* is not essential for sperm guidance (Fig. 1E and Table 1, line 4). To test whether *inx-22* affects INX-14 localization, we performed INX-14 immunostaining on *inx-22(tm1661)* null gonads. We found that INX-14 is in large part localized correctly in *inx-22(tm1661)* distal gonads (Fig. 2E, H, and K). However, INX-14 puncta at the sheath/oocyte interface in the proximal gonad are largely absent. Similar results were observed by T. Starich and D. Greenstein (unpublished data). Therefore, *inx-22* is essential for INX-14 localization in proximal gonads, but not in distal gonads. These results are consistent with genetic data: *inx-22* or *inx-14* loss causes precocious oocyte maturation, but only *inx-14* loss causes abnormal sperm guidance. Taken together, the genetic and localization data strongly support the hypothesis that INX-14 acts in the distal gonad to regulate sperm guidance.

Sheath cell contact is essential for INX-14-dependent sperm guidance

CEH-18 is a POU-class transcription factor that is expressed in sheath cells, but not in oocytes (Rose et al., 1997). In *ceh-18(mg57)* mutants, the interface between sheath cells and oocytes is expanded, disrupting contact-dependent signaling mechanisms (Rose et al., 1997; Whitten and Miller, 2007). To test whether sheath contact is essential for sperm guidance, we examined wild-type sperm distribution in *ceh-18(mg57)* null mutants one hour after mating. Sperm fail to accumulate efficiently at the spermatheca in *ceh-18(mg57)* mutants, although the defects are less severe than *inx-14(RNAi)* and *inx-14(ag17)* hermaphrodites (Fig. 1B–F; $P < 0.001$ for *ceh-18* mutants compared to control). Similar results are observed when sperm motility is measured within the uterus after mating (Table 1, lines 1–5; $P < 0.001$ for *ceh-18* mutants compared to control). Therefore, *ceh-18* loss causes sperm guidance defects. To test whether *ceh-18* is required for INX-14 localization, we stained *ceh-18(mg57)* mutant gonads with anti-INX-14 antibodies. No difference in INX-14 localization was observed (Fig. 2I–K; $P > 0.05$ compared to the control), suggesting that *ceh-18* loss simply disrupts germ cell/sheath cell contact. We considered the possibility that *inx-14* and *ceh-18* act in different pathways to regulate sperm guidance. However, *inx-14(RNAi)* in the *ceh-18(mg57)* null mutant background causes the same sperm guidance defects as *inx-14(RNAi)* alone (Fig. 1D and G; $P > 0.05$), a result consistent with *inx-14* and *ceh-18* acting in the same genetic pathway. These data support the hypothesis that sheath cell contact is critical for INX-14-dependent control of sperm guidance.

We considered two models to explain the current data. INX-14 in germ cells interacts with INX-14 in sheath cells or alternatively, INX-14 in germ cells interacts with another innexin in sheath cells. Support for the latter model comes from a genome-wide study of innexin promoters (Altun et al., 2009). The predicted promoter region of *inx-14* did not drive expression in sheath cells. However, predicted promoters for *inx-5*, *inx-8*, *inx-9*, and *inx-10* did drive sheath expression in the adult gonad. We screened these four innexins for sperm guidance defects and found strong defects in *inx-8(RNAi)* and *inx-9(RNAi)* hermaphrodites (Fig. 4A and data not shown; $P < 0.001$). *inx-5(RNAi)* and *inx-10(RNAi)* causes mild sperm accumulation defects (data not shown). *inx-8* and *inx-9* encode tightly linked paralogs that are 85% identical and RNAi of either gene is predicted to affect both mRNAs. To test whether these innexins act in germ cells or sheath cells, we used *rrf-1(pk1417)* mutants. The *rrf-1* gene encodes an RNA-dependent RNA polymerase that is required for RNAi in somatic sheath cells, but not in germ cells (Sijen et al., 2001). We have previously shown that the *rrf-1(pk1417)* mutation does not affect sperm guidance (Edmonds et al., 2010; Kubagawa et al., 2006). *inx-8(RNAi)* in the *rrf-1(pk1417)* background fails to cause sperm guidance defects, whereas *inx-8(RNAi)* in control hermaphrodites causes severe defects (Fig. 4A–C). In contrast, the sperm guidance defects in *inx-14(RNAi)* hermaphrodites (Fig. 1D) are similar to those in *inx-14(RNAi) rrf-1(pk1417)* hermaphrodites (Fig. 4D). These results support the hypothesis that *inx-14* functions in the germ line and *inx-8* (and *inx-9*) function

in sheath cells. Taken together, our results support the model that sheath to germ cell communication mediated by multiple innexins promotes sperm guidance to the spermatheca.

INX-14 promotes prostaglandin signaling

We have previously shown that oocytes secrete F-series prostaglandins to guide sperm to the spermatheca (Edmonds et al., 2010). Given that sperm used in our assays are wild-type, the defect in *inx-14(RNAi)* animals is likely to be upstream of the sperm signal transduction machinery. In mutant hermaphrodites deficient for oocyte prostaglandin production, sperm migrate through the uterus with reduced velocity, no directional velocity, and a high reversal frequency (Edmonds et al., 2010; Kubagawa et al., 2006). The sperm migration behavior in *inx-14(RNAi)* hermaphrodites is nearly identical to that in prostaglandin-deficient strains, suggesting that INX-14 promotes prostaglandin signaling to sperm. The RME-2 low-density lipoprotein receptor is specifically expressed in oocytes (Grant and Hirsh, 1999), where it is required to deliver prostaglandin PUFA precursors to oocytes in yolk lipoprotein complexes. In *rme-2(b1008)* mutants, oocytes fail to synthesize prostaglandins and sperm migrate with reduced velocity and directional velocity (Edmonds et al., 2010; Kubagawa et al., 2006). To investigate the genetic relationship between *inx-14* and *rme-2*, we compared sperm guidance in *rme-2(b1008)* null mutants to *inx-14(RNAi); rme-2(b1008)* mutants. *inx-14(RNAi)* does not influence the sperm guidance defects caused by *rme-2* loss, a result consistent with *inx-14* and *rme-2* acting in the same genetic pathway (Fig. 5A; $P > 0.05$). To directly test whether INX-14 affects prostaglandin signaling, we microinjected human PGF2α into the uterus of *inx-14(RNAi)* hermaphrodites mated to MT-labeled males (Fig. 5B). We have previously shown that PGF2α injection into prostaglandin-deficient mutants rescues the sperm velocity defects (Edmonds et al., 2010). Similarly, PGF2α injection into *inx-14(RNAi)* uteri rescues the sperm velocity defects (Fig. 5C; $P < 0.001$ compared to the control). We conclude that *inx-14* loss inhibits prostaglandin signaling in the uterus.

We sought to identify the step where INX-14 functions in the prostaglandin signaling mechanism. PUFA deficiency causes sperm guidance defects that can be rescued by exogenous PUFA supplementation (Kubagawa et al., 2006). PUFA supplementation did not rescue the sperm guidance defects of *inx-14(RNAi)*, *inx-14(ag17)*, and *ceh-18(mg57)* hermaphrodites (Fig. S2; $P > 0.05$), but it did rescue defects associated with *fat-2* loss (data not shown; *fat-2* is essential for PUFA synthesis). Therefore, *inx-14* signaling is not required for PUFA synthesis. Another possibility is that *inx-14* regulates PUFA transport to oocytes in yolk. To investigate this possibility, we examined oocyte yolk endocytosis in *inx-14(RNAi)* hermaphrodites using a *vit-2p::vit-2::gfp* transgene (YP170::GFP) (Grant and Hirsh, 1999). *vit-2* encodes an ApoB-100 homolog that is incorporated into yolk during its synthesis in the intestine. Oocyte yolk distribution in *inx-14(RNAi)* hermaphrodites is similar to yolk distribution in controls (Fig. 6). We did detect increased yolk in the pseudocoelom of *inx-14(RNAi)* animals, suggesting that yolk synthesis is increased or the total yolk endocytosis rate is decreased. *inx-14* or *ceh-18* loss does not influence fatty acid distribution in oocytes visualized using BODIPY-conjugated fatty acids (data not shown), indicating that fat transport to oocyte membranes still occurs. These data support the hypothesis that INX-14 is required for a step that occurs after PUFA metabolism and transport to oocytes.

Next, we tested whether *inx-14* regulates prostaglandin metabolism or stability. If *inx-14* is required for prostaglandin synthesis, *inx-14(ag17)* and *ceh-18(mg57)* mutant animals should have reduced levels of F-series prostaglandins synthesized by oocytes. Liquid chromatography electrospray ionization tandem mass spectrometry (LC-ESI-MS/MS) operated in multiple reaction monitoring (MRM) mode was utilized to measure specific prostaglandin analogs in worm lipid extracts (Edmonds et al., 2010). In this method, the parent mass of the carboxylate anion, together with the unique product ions derived from collisional activation in MRM experiments, confers high specificity and sensitivity (Murphy

et al., 2005). Previously, we used MRM with mass transition *m/z* 353/193 to identify a $PGF_{2\alpha}$ isomer called CePGF2 and structurally-related prostaglandins synthesized by oocytes (Edmonds et al., 2010). We found that CePGF2 and other $PGF_{2\alpha}$ analogs are increased in *inx-14(ag17)* mutant extracts relative to wild-type extracts (Fig. 5D). Similar results are observed using MRM with mass transition *m/z* 351/191, which detects PGF_3-like compounds derived from eicosapentaenoic acid (Fig. 5E). These data suggest that INX-14 regulates F-series prostaglandin metabolism, either by inhibiting synthesis or promoting catabolism. Although CePGF2 levels in *ceh-18(mg57)* mutant extracts are similar to those in wild-type extracts, DAF-16 is down-regulating prostaglandin synthesis in these mutants (see below). Taken together, the data support the model that INX-14 promotes prostaglandin signaling, possibly at the level of prostaglandin transport (see Discussion).

Sheath cell/germ cell signaling inhibits DAF-16/FOXO transcription factor activity

Our data provide strong evidence that INX-14 functions in oocyte precursors. A major difference between oocyte precursors in the distal gonad and oocytes in the proximal gonad is that the former are transcriptionally active and latter are not (Kelly et al., 2002; Schisa et al., 2001; Seydoux and Dunn, 1997). These data raise the possibility that INX-14 acts in oocyte precursors to regulate gene transcription essential for prostaglandin signaling. A previous study showed that *inx-14*, *inx-8*, or *inx-9* loss (but not other innexins) causes increased DAF-16/FOXO transcriptional activity (Miyata et al., 2008), which inhibits prostaglandin signaling and sperm guidance (Edmonds et al., 2010). To further investigate this mechanism, we used transgenic strains that drive GFP expression under control of the *sod-3* promoter, a direct downstream target of DAF-16 (Henderson et al., 2006; Oh et al., 2006). As previously reported, *sod-3* expression is mildly up-regulated in *inx-14(RNAi)* hermaphrodites and *inx-14(ag17)* hermaphrodites (Fig. 7). We also found that *ceh-18(mg57)* hermaphrodites have elevated DAF-16-dependent transcriptional activity throughout the body (Fig. 7). We considered the possibility that *ceh-18* represses DAF-16 by a mechanism similar to *fat-2* (Edmonds et al., 2010). However, in contrast to *fat-2(wa17)* mutants, arachidonic acid supplementation does not suppress the elevated DAF-16 activity in *ceh-18(mg57)* mutants (Fig. 7). These data suggest that sheath/germ cell interactions via innexins inhibit DAF-16.

We previously showed that DAF-16 inactivation partially suppresses the sperm guidance defects in *daf-2* insulin receptor mutants (Edmonds et al., 2010). To directly assess the role of DAF-16 in INX-14-mediated sperm guidance, we examined *inx-14(RNAi) daf-16(mu86)* and *ceh-18(mg57); daf-16(mu86)* null mutant hermaphrodites. *daf-16* loss does not suppress the sperm guidance defects caused by *inx-14* or *ceh-18* loss (Fig 8A-D). Furthermore, *daf-16* loss does not affect fertilized egg production in *ceh-18(mg57)* hermaphrodites (Fig. 8E; $P > 0.05$). We found a slight increase in the number of fertilized eggs laid in *inx-14(RNAi) daf-16(mu86)* hermaphrodites compared to *inx-14(RNAi)* hermaphrodites, suggesting that DAF-16 does weakly inhibit total fertility (Fig. 8E; $P = 0.005$). These data indicate that INX-14 promotes sperm guidance independent of DAF-16 or at a step downstream of DAF-16. We previously reported that DAF-16 inhibits CePGF2 synthesis in *daf-2* mutants (Edmonds et al., 2010). Indeed, MRM with mass transition *m/z* 353/*193* shows that CePGF2 levels are elevated in *ceh-18(mg57); daf-16(mu86*) mutant extracts relative to *ceh-18(mg57)* mutant extracts (Fig. 5F). Thus, increasing prostaglandin synthesis in *ceh-18* mutants through DAF-16 inactivation does not affect sperm guidance.

Discussion

Here we provide evidence that the gap junctional subunit INX-14 functions in oocyte precursors in the adult distal gonad to promote sperm guidance to the fertilization site. These results, along with those of previous studies (Edmonds et al., 2010; Kubagawa et al., 2006),

support the following model. When food is available, insulin signaling stimulates PUFA transport from the intestine to oocytes in yolk lipoprotein complexes. Oocyte PUFAs are converted into F-series prostaglandins, which are transported into the reproductive tract extracellular environment. These prostaglandins stimulate the guidance of self-derived and male-derived sperm toward the spermatheca. During oocyte development, a somatic gonad/germ cell signaling pathway mediated by INX-14 in germ cells and INX-8/INX-9 in sheath cells regulates gene transcription or an alternative process essential for prostaglandin transport or function in the proximal gonad. Thus, communication between germ line and soma promotes prostaglandin signaling critical for sperm function.

Genetic and immuno-localization data strongly support the model that INX-14 acts in the distal gonad. Why might INX-14 function in oocyte precursors rather than differentiated oocytes to promote sperm guidance? A possible mechanism involves transcriptional regulation. Oocytes in the proximal gonad cease transcribing mRNA during diakinesis and remain transcriptionally silent until embryonic development (Kelly et al., 2002; Schisa et al., 2001; Seydoux and Dunn, 1997). Therefore, mRNAs needed for fertilization must be transcribed earlier in development. Consistent with this explanation, *inx-14* and *inx-8/inx-9* regulate DAF-16 transcriptional activity (Miyata et al., 2008) that inhibits oocyte prostaglandin synthesis (Edmonds et al., 2010). However, DAF-16 is not the principal mechanism by which INX-14 promotes sperm guidance. One model is that INX-14 signaling regulates DAF-16-dependent and DAF-16-independent transcriptional mechanisms that promote sperm guidance, with the latter acting downstream of prostaglandin synthesis. Another model is that the elevated DAF-16 activity observed in *inx-14* and *ceh-18* mutants is not directly related to INX-14 signaling. In any event, INX-14 signaling in oocyte precursors could regulate gene transcription. Transcription-independent mechanisms are also possible, including those that control the flow of molecules from germ cells through the rachis into differentiating oocytes.

Our data provide evidence that sheath and germ cell contact mediated by innexins in the distal gonad promotes sperm guidance. However, transmission and freeze fracture electron microscopy has yet to detect gap junctions in this region (Hall et al., 1999). INX-14 puncta at the sheath/germ cell interface look similar to puncta at the sheath/oocyte interface in the proximal gonad, where gap junctions have been detected. Based on current data, there are two possibilities. INX-14 mediates the assembly of gap junctions in the distal gonad that are difficult to document. In this case, molecules flowing through the channels are predicted to initiate transduction events that regulate gene expression. Alternatively, innexin-dependent contact between sheath cells and germ cells induces signal transduction independent of channel formation. The latter possibility excludes mechanisms whereby molecules are transferred from sheath to germ cells. In this case, conformational changes or adhesion mediated by innexin contact might initiate signal transduction.

Genetic and microinjection experiments support the model that INX-14 is required for prostaglandin signaling at a step downstream of F-series prostaglandin synthesis. Wild-type sperm in *inx-14* mutant hermaphrodite uteri behave as though prostaglandins are not present, yet levels of CePGF2 and other prostaglandins synthesized largely by oocytes are elevated. A possible explanation for these data is that INX-14 affects prostaglandin transport. Inhibiting prostaglandin accumulation in the extracellular environment is likely to cause reduced prostaglandin catabolism and sperm guidance. The mechanism by which prostaglandins are released from cells is not well understood, but may involve passive diffusion or members of the ATP-binding cassette (ABC) transporter family of membrane export pumps. The ABC transporter MRP4 mediates the uptake of PGE_1 and PGE_2 into insect and HEK293 cell membranes (Reid et al., 2003). We previously identified two ABC transporters that function in the germ line to promote sperm guidance (Kubagawa et al.,

2006). Whether INX-14 regulates the expression of these transporters and whether they export prostaglandins are not known. In addition to ABC transporters, the *C. elegans* genome encodes predicted prostaglandin transporters, which mediate the cellular uptake of prostaglandins (Kanai et al., 1995; Schuster, 2002). Another possibility independent of transport is that INX-14 promotes the conversion of CePGF2 and related prostaglandins into more potent prostaglandins that are the "true" active factors. However, human $PGF_{2\alpha}$ is effective in stimulating sperm migration at nanomolar concentrations (Edmonds et al., 2010). Sperm motility behavior in *inx-14(RNAi)* hermaphrodite uteri is nearly identical to their behavior in prostaglandin-deficient uteri, although CePGF2 is synthesized. Moreover, increasing prostaglandin synthesis in *ceh-18* and *inx-14* mutants through DAF-16 inactivation does not rescue the sperm guidance defects. Given these results, the elevated F-series prostaglandin levels in *inx-14(ag17)* mutants are more consistent with a transport defect that inhibits catabolism, but a role in synthesis of a late product cannot be excluded. It is also possible that the elevated prostaglandin levels seen in the *inx-14* mutant extracts are due to increased synthesis in non-gonadal tissues. Distinguishing among these possibilities will require identification of downstream targets of INX-14 signaling.

There are surprising similarities in the expression patterns and functions of mammalian connexins/pannexins and *C. elegans* innexins in the ovary. In mammals, five connexins and the pannexin PANX1 are expressed in oocytes or the surrounding follicle cells (Baranova et al., 2004; Kidder and Mhawi, 2002). Gap junctions have been reported between oocytes and follicle cells, as well as between follicle cells (Anderson and Albertini, 1976; Gilula et al., 1978). Genetic and biochemical studies have documented roles for connexins in follicle development and oocyte maturation (Gittens and Kidder, 2005; Simon et al., 1997). In *C. elegans*, six innexins are expressed in the germ line or surrounding sheath cells (Altun et al., 2009; Govindan et al., 2009). Gap junctions have been reported between oocytes and sheath cells, as well as between the sheath cells themselves (Hall et al., 1999; Whitten and Miller, 2007). *inx-14* null mutants have germ cell development and differentiation defects (Govindan et al., 2009). INX-14 and INX-22 are expressed in developing germ cells and oocytes, where they inhibit precocious oocyte maturation (Govindan et al., 2006; Whitten and Miller, 2007). These data raise the possibility that gap junctional subunits have conserved functions in invertebrates and vertebrates, despite limited sequence similarity.

Whether gap junctions regulate sperm guidance in mammals is not clear. Little is known about the mechanisms that control mammalian sperm guidance *in vivo*. Growing *in vitro* evidence suggests that mammalian sperm respond to multiple chemoattractants secreted by ovulated oocytes and cumulus cells, called cumulus masses (Eisenbach and Giojalas, 2006). Among the molecules secreted by cumulus masses are progesterone and prostaglandins (Lim et al., 1997; Murdoch et al., 1993). *in vitro* chemotaxis assays have shown that progesterone is capable of attracting sperm at picomolar concentrations (Guidobaldi et al., 2008; Teves et al., 2006). Although there have been sporadic reports that prostaglandins can influence sperm head rotation and velocity (Aitken and Kelly, 1985; Gottlieb et al., 1988), it is not clear whether prostaglandins can attract sperm *in vitro*. Prostaglandin-deficient mice have fertilization defects that could be due in part to abnormal sperm guidance (Lim et al., 1997; Tamba et al., 2008). Of particular interest are two recent studies showing that progesterone and prostaglandins bind to distinct sites to activate CatSper, a pH-dependent calcium channel in the mammalian sperm flagellum implicated in chemotaxis (Lishko et al., 2011; Strunker et al., 2011). In *C. elegans*, sterols do not appear to be necessary for sperm guidance, but prostaglandins are necessary (Edmonds et al., 2010; Kubagawa et al., 2006). *C. elegans* sperm travel up to three hundred microns to reach ovulated oocytes, whereas this distance in mammals is much greater. Greater distances may require multiple chemoattractants to ensure that sperm find oocytes efficiently. An interesting difference between nematode sperm and mammalian sperm is the motility apparatus, a pseudopod

instead of a flagellum (Bottino et al., 2002; Han et al., 2010; L'Hernault, 2009). While there are obvious differences between *C. elegans* and mammalian systems, a picture is emerging in which some molecular mechanisms may be evolutionarily conserved. Delineating conserved versus derived mechanisms should lead to better understanding of those that are fundamental to animal reproduction.

In summary, we provide strong evidence that somatic sheath cells communicate with developing germ cells in the adult distal gonad to promote sperm guidance. This communication mechanism is mediated by multiple innexins, including INX-14 in oocyte precursors. INX-14 promotes prostaglandin signaling in the uterus, possibly by regulating the transcription of a factor(s) important for prostaglandin transport or function. Future work will be necessary to test this model and fully delineate the mechanism(s) by which INX-14 controls sperm guidance.

Experimental Procedures

C. elegans Strains and RNA-mediated Interference

C. elegans strains were maintained at 16, 20, or 25°C, as indicated. Males used for sperm guidance assays were generated with the *fog-2(q71)* strain, which maintains a stable male/female population by feminizing the hermaphrodite germ line (Schedl and Kimble, 1988). The following lines were used: N2 Bristol (wild type), CB4108 [*fog-2(q71)V*], AU98 [*inx-14(ag17)I*], NL2098 [*rrf-1(pk1417)I*], XM1011 [*inx-22(tm1661)I*], GR1034 [*ceh-18(mg57)X*], BX26 [*fat-2(wa17)IV*], CF1038 [*daf-16(mu86)I*], KG532 [*kin-2(ce179)X*], MT2426 [*goa-1(n1134)I*], *inx-14(ag17)I; fog-2(q71)V*, *ceh-18(mg57)X; fog-2(q71)V*, and *ceh-18(mg57)X; daf-16(mu86)I*. Transgenic strain *bIs1(vit-2p::vit-2::GFP)* expresses a fusion of the yolk protein YP170 and GFP (Grant and Hirsh, 1999). RNAi was performed using the feeding method (Timmons and Fire, 1998). HT115 bacterial strains were obtained from the feeding library and confirmed for the presence of the correct target (Kamath and Ahringer, 2003).

MitoTracker Staining and Sperm Guidance Assays

MitoTracker Red CMXRos (Invitrogen) dye, which selectively stains mitochondria, was used for labeling *fog-2(q71)* male sperm, as previously described (Edmonds et al., 2010; Kubagawa et al., 2006). MitoTracker does not affect sperm function or motility. 100–150 males were transferred to a watchglass containing 10 μM MitoTracker in 300 μl M9 buffer (1% DMSO). Males were incubated in the dark for 2 hours, transferred to an NGM plate seeded with *E. coli* for 2–3 hours, and then transferred to a fresh NGM plate overnight. For sperm guidance assays, 15–20 adult hermaphrodites, approximately 24–36 hours post L4 stage, were anesthetized in a solution of 0.1% tricaine and 0.01% tetramisole hydrochloride in M9 buffer for 30 minutes. Anesthetized adults were carefully transferred to a 0.5 cm diameter bacterial spot on an NGM plate containing 50–75 MitoTracker-stained males. Animals were allowed to mate for 30 minutes. The mated hermaphrodites were gently transferred to a 2% agarose pad on a microscope slide and mounted for microscopy. Imaging was performed on a Zeiss Axioskop 2 plus equipped with epi-fluorescence, a 63X objective, MRM Axiocam Hi-Res digital camera, PC computer, and Axiovision software. For sperm guidance analysis, both DIC and fluorescent images were taken every 30 seconds. Axiovision software was used to measure sperm migration distances through the uterus for a minimum of 6 consecutive frames. The uterus of each gonad was measured from the vulva to the distal end of the spermatheca and divided into three zones – the spermatheca, middle, and vulval zones. Sperm motility was measured in the middle zone. Average velocity is calculated as the total distance traveled by a single sperm divided by time. Vectorial velocity is the distance that sperm migrate toward the spermatheca (along a straight line drawn

through the anteroposterior axis of the uterus) divided by time. Reversals were defined as a change in sperm direction of greater than 90° over three subsequent frames.

For sperm accumulation experiments, anesthetized hermaphrodites were mated to MitoTracker stained males for 30 minutes before transferring to a seeded recovery plate for one hour. Control experiments show that by one hour after transferring, greater than 90% of wild-type sperm accumulate at the spermatheca (Edmonds et al., 2010). Fluorescence images were taken to document sperm distribution within the uterus. Sperm were counted in each zone and divided by the total number of sperm in all three zones.

Antibody Staining

Immunocytochemistry on dissected gonads using anti-INX-14 antibodies was performed as previously described (Govindan et al., 2009).

Fatty Acid Supplementation

PUFA-containing NGM plates were prepared as previously described (Kubagawa et al., 2006; Watts and Browse, 2002). Briefly, arachidonic acid was added to liquid NGM at a temperature of less than 50°C very slowly until mixed thoroughly to a final concentration of 100–200 μM. Plates were kept in the dark and seeded with NA22 bacteria after 24 hours. The bacterial lawn was allowed to grow in the dark for 2–3 days before use. Bacteria accumulate PUFAs in their membranes as they grow on the NGM plates at ranges from 1–5% (Kubagawa et al., 2006). Worms were allowed to grow on PUFA-containing plates for 1–2 generations. *sod-3p::GFP* images were taken using identical exposure times.

Microinjections

Human $PGF_{2\alpha}$ (Cayman Chemical) was microinjected through the vulva and into the uterus of *inx-14(RNAi)* hermaphrodites immediately after mating to MitoTracker-stained males (Edmonds et al., 2010). Fresh nitrogen-purged $PGF_{2\alpha}$ was dissolved in ethanol and diluted in M9 buffer to a final concentration of 25 μM and 5% ethanol. The solution was loaded in a needle and injected using a Zeiss Axiovert 200 microscope, hydraulic fine type micromanipulator, and Narishige IM-30 microinjector. After injection, hermaphrodites were allowed to recover for 5 minutes in M9 buffer + ~500 mM NaCl to minimize expulsion of the uterus through the vulva. Time-lapse videos were taken immediately after the 5 min recovery to limit the risk of prostaglandin metabolism.

Lipid Extraction

A mixed-stage culture of each strain was grown on four 150 mm NGM plates seeded with NA22 bacteria. After the worms reached high density, they were washed from the plates with M9 buffer, resuspended in 60 mls of M9, and distributed into 1 ml aliquots to 60 seeded 150 mm NGM plates. Worms were grown for approximately 3 generations. *inx-14(ag17)* and control hermaphrodites were grown at 20°C for the first two generations and then switched to 25°C for 36 hours before harvesting. Worms were grown at 20°C for other experiments. During their growth, worms were supplemented with concentrated NA22 bacteria to prevent starvation. The worms were washed from plates with M9 buffer, washed 2 additional times, and pelleted in a clinical centrifuge at 2500 RPM. M9 was removed and the pellet was frozen at −80°C. Each 60-plate culture yielded at least 6 grams of tissue.

For lipid extraction, tissue was weighed to ensure that equal amounts were used for extraction. Individual samples differed by less than 1% total mass. The vast majority of tissue in these cultures was from adult hermaphrodites. Lipids were extracted using a modified mammalian PG extraction protocol (Edmonds et al., 2010; Golovko and Murphy, 2008). The ~6 grams of frozen worm tissue from each strain was thawed and thoroughly

mixed with 12 ml of 2:1 acetone:saline solution using a glass rod. 1.5 ml of resuspended tissue was aliquotted into 12.5 ml tubes. 0.5 ml of 0.5 mm diameter zirconium oxide beads were added to each tube, the tubes were capped, and tissue was homogenized in a Bullet Blender 5 (NextAdvance, Inc.) for 2 minutes at speed 8. Homogenized tissue was transferred to clean 15 ml conicals, the tissue and zirconium oxide beads were pelleted, and the supernatant was removed.

For extraction of PGs, the supernatant was divided evenly between 4 silicanized (Sigmacote, Sigma Aldrich) 10 ml glass tubes. 3 ml hexane was added to each tube, the tubes were vortexed for 30 seconds, and the samples were spun down at 4°C for 10 minutes at 3500 RPM. The upper hexane phase was discarded. The lower phase was acidified with ~100 ul of 2 M formic acid to a pH of 3.5. 3 ml of chloroform was added to each tube and the samples were vortexed for 30 seconds, followed by a spin at 4°C for 10 minutes at 3500 RPM. The lower PG-containing chloroform phase was removed from each tube and combined in a single 15 ml silicanized glass tube. The sample was placed at −20°C overnight to ensure complete separation of chloroform and aqueous phases. The purified chloroform phase was then dried under nitrogen gas, and the dried lipids were stored in a nitrogen-purged glass vial at −20°C until analysis by mass spectrometry. The samples were reconstituted in 200 μl of methanol:water (8:2 v/v) for LC-ESI-MS/MS analysis.

Mass Spectrometry

LC-ESI-MS/MS analyses of *C. elegans* extracts were performed as previously described (Edmonds et al., 2010). Briefly, LC-ESI-MS/MS analyses of PG standards and the methanolic extracts of *C. elegans* were performed using a system consisting of a Shimadzu Prominence HPLC with a refrigerated auto sampler (Shimadzu Scientific Instruments, Inc. Columbia, MD), and an API 4000 (Applied Biosystems/MDS Sciex, Concord, Ontario, Canada) triple quadrupole mass spectrometer. The chromatographic separation was performed on a Synergy hydro RP-C18 column (250 × 2.0 mm i.d) pre-equilibrated with 0.1% formic acid. The mobile phase consists of 0.1% formic acid [A] and acetonitrile containing 0.1% formic acid [B] and was pumped at a flow rate of 0.2 mL/min. The gradient started with 10% B and went up to 80% B from 0–11 min, 80–100% B from 11–14 min and returned back to 10% B at 16 min. The MRM analysis was conducted by monitoring the precursor ion to product ion transitions from *m/z* 353/193 (PGF2α), 351/189 (PGD2, PGE2), 351/191 (PGF3α–l). The LC-MS/MS system was controlled by Analyst 1.4.2 software.

Supplementary Material

Refer to Web version on PubMed Central for supplementary material.

Acknowledgments

We thank T. Starich and D. Greenstein for the anti-INX-14 antibodies, sharing unpublished data, and comments on the manuscript. We also thank Chenbei Chang for help with unpublished Xenopus experiments and the UAB Targeted Metabolomics and Proteomics Laboratory, which has been supported in part by an NCI Core Research Support Grant to the UAB Comprehensive Cancer. Some strains were provided by the *Caenorhabditis* Genetics Center, which is funded by the NIH. This work was supported by the NIH NIGMS (R01GM085105 to MAM, including an ARRA administrative supplement) and an American Cancer Society Research Scholars Grant (RSG-06-151-01-DDC to MAM). Additional support came from the UAB Division of Reproductive Endocrinology and Infertility, Department of Obstetrics and Gynecology.

References

Ackert CL, Gittens JE, O'Brien MJ, Eppig JJ, Kidder GM. Intercellular communication via connexin43 gap junctions is required for ovarian folliculogenesis in the mouse. Dev Biol. 2001; 233:258–70. [PubMed: 11336494]

Aitken RJ, Kelly RW. Analysis of the direct effects of prostaglandins on human sperm function. J Reprod Fertil. 1985; 73:139–46. [PubMed: 3855460]

Altun ZF, Chen B, Wang ZW, Hall DH. High resolution map of Caenorhabditis elegans gap junction proteins. Dev Dyn. 2009; 238:1936–50. [PubMed: 19621339]

Anderson E, Albertini DF. Gap junctions between the oocyte and companion follicle cells in the mammalian ovary. J Cell Biol. 1976; 71:680–6. [PubMed: 825522]

Baranova A, Ivanov D, Petrash N, Pestova A, Skoblov M, Kelmanson I, Shagin D, Nazarenko S, Geraymovych E, Litvin O, Tiunova A, Born TL, Usman N, Staroverov D, Lukyanov S, Panchin Y. The mammalian pannexin family is homologous to the invertebrate innexin gap junction proteins. Genomics. 2004; 83:706–16. [PubMed: 15028292]

Bevans CG, Kordel M, Rhee SK, Harris AL. Isoform composition of connexin channels determines selectivity among second messengers and uncharged molecules. J Biol Chem. 1998; 273:2808–16. [PubMed: 9446589]

Bottino D, Mogilner A, Roberts T, Stewart M, Oster G. How nematode sperm crawl. J Cell Sci. 2002; 115:367–84. [PubMed: 11839788]

Dbouk HA, Mroue RM, El-Sabban ME, Talhouk RS. Connexins: a myriad of functions extending beyond assembly of gap junction channels. Cell Commun Signal. 2009; 7:4. [PubMed: 19284610]

Dekel N. Cellular, biochemical and molecular mechanisms regulating oocyte maturation. Mol Cell Endocrinol. 2005; 234:19–25. [PubMed: 15836949]

Edmonds JW, Prasain JK, Dorand D, Yang Y, Hoang HD, Vibbert J, Kubagawa HM, Miller MA. Insulin/FOXO signaling regulates ovarian prostaglandins critical for reproduction. Dev Cell. 2010; 19:858–71. [PubMed: 21145501]

Eisenbach M, Giojalas LC. Sperm guidance in mammals - an unpaved road to the egg. Nat Rev Mol Cell Biol. 2006; 7:276–85. [PubMed: 16607290]

Gershon E, Plaks V, Dekel N. Gap junctions in the ovary: expression, localization and function. Mol Cell Endocrinol. 2008; 282:18–25. [PubMed: 18162286]

Gilula NB, Epstein ML, Beers WH. Cell-to-cell communication and ovulation. A study of the cumulus-oocyte complex. J Cell Biol. 1978; 78:58–75. [PubMed: 670298]

Gittens JE, Kidder GM. Differential contributions of connexin37 and connexin43 to oogenesis revealed in chimeric reaggregated mouse ovaries. J Cell Sci. 2005; 118:5071–8. [PubMed: 16254245]

Golovko MY, Murphy EJ. An improved LC-MS/MS procedure for brain prostanoid analysis using brain fixation with head-focused microwave irradiation and liquid-liquid extraction. J Lipid Res. 2008; 49:893–902. [PubMed: 18187404]

Goodenough DA. Bulk isolation of mouse hepatocyte gap junctions. Characterization of the principal protein, connexin. J Cell Biol. 1974; 61:557–63. [PubMed: 4363961]

Gottlieb C, Svanborg K, Eneroth P, Bygdeman M. Effect of prostaglandins on human sperm function in vitro and seminal adenosine triphosphate content. Fertil Steril. 1988; 49:322–7. [PubMed: 3338588]

Govindan JA, Cheng H, Harris JE, Greenstein D. Galphao/i and Galphas signaling function in parallel with the MSP/Eph receptor to control meiotic diapause in C. elegans. Curr Biol. 2006; 16:1257–68. [PubMed: 16824915]

Govindan JA, Nadarajan S, Kim S, Starich TA, Greenstein D. Somatic cAMP signaling regulates MSP-dependent oocyte growth and meiotic maturation in C. elegans. Development. 2009; 136:2211–21. [PubMed: 19502483]

Grant B, Hirsh D. Receptor-mediated endocytosis in the Caenorhabditis elegans oocyte. Mol Biol Cell. 1999; 10:4311–26. [PubMed: 10588660]

Guidobaldi HA, Teves ME, Unates DR, Anastasia A, Giojalas LC. Progesterone from the cumulus cells is the sperm chemoattractant secreted by the rabbit oocyte cumulus complex. PLoS One. 2008; 3:e3040. [PubMed: 18725941]

Hall DH, Winfrey VP, Blaeuer G, Hoffman LH, Furuta T, Rose KL, Hobert O, Greenstein D. Ultrastructural features of the adult hermaphrodite gonad of Caenorhabditis elegans: relations between the germ line and soma. Dev Biol. 1999; 212:101–23. [PubMed: 10419689]

Han SM, Cottee PA, Miller MA. Sperm and oocyte communication mechanisms controlling C. elegans fertility. Dev Dyn. 2010; 239:1265–81. [PubMed: 20034089]

Harris AL. Emerging issues of connexin channels: biophysics fills the gap. Q Rev Biophys. 2001; 34:325–472. [PubMed: 11838236]

Henderson ST, Bonafe M, Johnson TE. daf-16 protects the nematode Caenorhabditis elegans during food deprivation. J Gerontol A Biol Sci Med Sci. 2006; 61:444–60. [PubMed: 16720740]

Juneja SC, Barr KJ, Enders GC, Kidder GM. Defects in the germ line and gonads of mice lacking connexin43. Biol Reprod. 1999; 60:1263–70. [PubMed: 10208994]

Kamath RS, Ahringer J. Genome-wide RNAi screening in Caenorhabditis elegans. Methods. 2003; 30:313–21. [PubMed: 12828945]

Kanai N, Lu R, Satriano JA, Bao Y, Wolkoff AW, Schuster VL. Identification and characterization of a prostaglandin transporter. Science. 1995; 268:866–9. [PubMed: 7754369]

Kelly WG, Schaner CE, Dernburg AF, Lee MH, Kim SK, Villeneuve AM, Reinke V. X-chromosome silencing in the germline of C. elegans. Development. 2002; 129:479–92. [PubMed: 11807039]

Kidder GM, Mhawi AA. Gap junctions and ovarian folliculogenesis. Reproduction. 2002; 123:613–20. [PubMed: 12006089]

Kubagawa HM, Watts JL, Corrigan C, Edmonds JW, Sztul E, Browse J, Miller MA. Oocyte signals derived from polyunsaturated fatty acids control sperm recruitment in vivo. Nat Cell Biol. 2006; 8:1143–8. [PubMed: 16998478]

L'Hernault SW. The genetics and cell biology of spermatogenesis in the nematode C. elegans. Mol Cell Endocrinol. 2009; 306:59–65. [PubMed: 19481685]

Lim H, Paria BC, Das SK, Dinchuk JE, Langenbach R, Trzaskos JM, Dey SK. Multiple female reproductive failures in cyclooxygenase 2-deficient mice. Cell. 1997; 91:197–208. [PubMed: 9346237]

Lishko PV, Botchkina IL, Kirichok Y. Progesterone activates the principal Ca2+ channel of human sperm. Nature. 2011; 471:387–91. [PubMed: 21412339]

Miller MA, Nguyen VQ, Lee MH, Kosinski M, Schedl T, Caprioli RM, Greenstein D. A sperm cytoskeletal protein that signals oocyte meiotic maturation and ovulation. Science. 2001; 291:2144–7. [PubMed: 11251118]

Miyata S, Begun J, Troemel ER, Ausubel FM. DAF-16-dependent suppression of immunity during reproduction in Caenorhabditis elegans. Genetics. 2008; 178:903–18. [PubMed: 18245330]

Mroue RM, El-Sabban ME, Talhouk RS. Connexins and the gap in context. Integr Biol (Camb). 2011; 3:255–66. [PubMed: 21437329]

Murdoch WJ, Hansen TR, McPherson LA. A review--role of eicosanoids in vertebrate ovulation. Prostaglandins. 1993; 46:85–115. [PubMed: 8210447]

Murphy RC, Barkley RM, Zemski Berry K, Hankin J, Harrison K, Johnson C, Krank J, McAnoy A, Uhlson C, Zarini S. Electrospray ionization and tandem mass spectrometry of eicosanoids. Anal Biochem. 2005; 346:1–42. [PubMed: 15961057]

Nicholson BJ. Gap junctions - from cell to molecule. J Cell Sci. 2003; 116:4479–81. [PubMed: 14576341]

Niessen H, Harz H, Bedner P, Kramer K, Willecke K. Selective permeability of different connexin channels to the second messenger inositol 1,4,5-trisphosphate. J Cell Sci. 2000; 113 (Pt 8):1365–72. [PubMed: 10725220]

Oh SW, Mukhopadhyay A, Dixit BL, Raha T, Green MR, Tissenbaum HA. Identification of direct DAF-16 targets controlling longevity, metabolism and diapause by chromatin immunoprecipitation. Nat Genet. 2006; 38:251–7. [PubMed: 16380712]

Panchin YV. Evolution of gap junction proteins--the pannexin alternative. J Exp Biol. 2005; 208:1415–9. [PubMed: 15802665]

Phelan P, Bacon JP, Davies JA, Stebbings LA, Todman MG, Avery L, Baines RA, Barnes TM, Ford C, Hekimi S, Lee R, Shaw JE, Starich TA, Curtin KD, Sun YA, Wyman RJ. Innexins: a family of invertebrate gap-junction proteins. Trends Genet. 1998; 14:348–9. [PubMed: 9769729]

Phelan P, Starich TA. Innexins get into the gap. Bioessays. 2001; 23:388–96. [PubMed: 11340620]

Reaume AG, de Sousa PA, Kulkarni S, Langille BL, Zhu D, Davies TC, Juneja SC, Kidder GM, Rossant J. Cardiac malformation in neonatal mice lacking connexin43. Science. 1995; 267:1831–4. [PubMed: 7892609]

Reid G, Wielinga P, Zelcer N, van der Heijden I, Kuil A, de Haas M, Wijnholds J, Borst P. The human multidrug resistance protein MRP4 functions as a prostaglandin efflux transporter and is inhibited by nonsteroidal antiinflammatory drugs. Proc Natl Acad Sci U S A. 2003; 100:9244–9. [PubMed: 12835412]

Rose KL, Winfrey VP, Hoffman LH, Hall DH, Furuta T, Greenstein D. The POU gene ceh-18 promotes gonadal sheath cell differentiation and function required for meiotic maturation and ovulation in Caenorhabditis elegans. Dev Biol. 1997; 192:59–77. [PubMed: 9405097]

Schedl T, Kimble J. fog-2, a germ-line-specific sex determination gene required for hermaphrodite spermatogenesis in Caenorhabditis elegans. Genetics. 1988; 119:43–61. [PubMed: 3396865]

Schisa JA, Pitt JN, Priess JR. Analysis of RNA associated with P granules in germ cells of C. elegans adults. Development. 2001; 128:1287–98. [PubMed: 11262230]

Schuster VL. Prostaglandin transport. Prostaglandins Other Lipid Mediat. 2002; 68–69:633–47.

Seydoux G, Dunn MA. Transcriptionally repressed germ cells lack a subpopulation of phosphorylated RNA polymerase II in early embryos of Caenorhabditis elegans and Drosophila melanogaster. Development. 1997; 124:2191–201. [PubMed: 9187145]

Sijen T, Fleenor J, Simmer F, Thijssen KL, Parrish S, Timmons L, Plasterk RH, Fire A. On the role of RNA amplification in dsRNA-triggered gene silencing. Cell. 2001; 107:465–76. [PubMed: 11719187]

Simon AM, Goodenough DA, Li E, Paul DL. Female infertility in mice lacking connexin 37. Nature. 1997; 385:525–9. [PubMed: 9020357]

Starich T, Sheehan M, Jadrich J, Shaw J. Innexins in C. elegans. Cell Commun Adhes. 2001; 8:311–4. [PubMed: 12064609]

Strunker T, Goodwin N, Brenker C, Kashikar ND, Weyand I, Seifert R, Kaupp UB. The CatSper channel mediates progesterone-induced Ca2+ influx in human sperm. Nature. 2011; 471:382–6. [PubMed: 21412338]

Tamba S, Yodoi R, Segi-Nishida E, Ichikawa A, Narumiya S, Sugimoto Y. Timely interaction between prostaglandin and chemokine signaling is a prerequisite for successful fertilization. Proc Natl Acad Sci U S A. 2008; 105:14539–44. [PubMed: 18794532]

Teves ME, Barbano F, Guidobaldi HA, Sanchez R, Miska W, Giojalas LC. Progesterone at the picomolar range is a chemoattractant for mammalian spermatozoa. Fertil Steril. 2006; 86:745–9. [PubMed: 16784744]

Timmons L, Fire A. Specific interference by ingested dsRNA. Nature. 1998; 395:854. [PubMed: 9804418]

Unger VM, Kumar NM, Gilula NB, Yeager M. Three-dimensional structure of a recombinant gap junction membrane channel. Science. 1999; 283:1176–80. [PubMed: 10024245]

Watts JL, Browse J. Genetic dissection of polyunsaturated fatty acid synthesis in Caenorhabditis elegans. Proc Natl Acad Sci U S A. 2002; 99:5854–9. [PubMed: 11972048]

Whitten SJ, Miller MA. The role of gap junctions in Caenorhabditis elegans oocyte maturation and fertilization. Dev Biol. 2007; 301:432–446. [PubMed: 16982048]

Yamamoto I, Kosinski ME, Greenstein D. Start me up: Cell signaling and the journey from oocyte to embryo in C. elegans. Dev Dyn. 2005

Highlights

- The gap junction subunit INX-14 acts in oocyte precursors to promote sperm guidance
- INX-14 loss causes sperm migration velocity and directional velocity defects
- Somatic gonadal sheath cell interaction is necessary for INX-14 function
- INX-14 promotes prostaglandin signaling to sperm that regulates motility

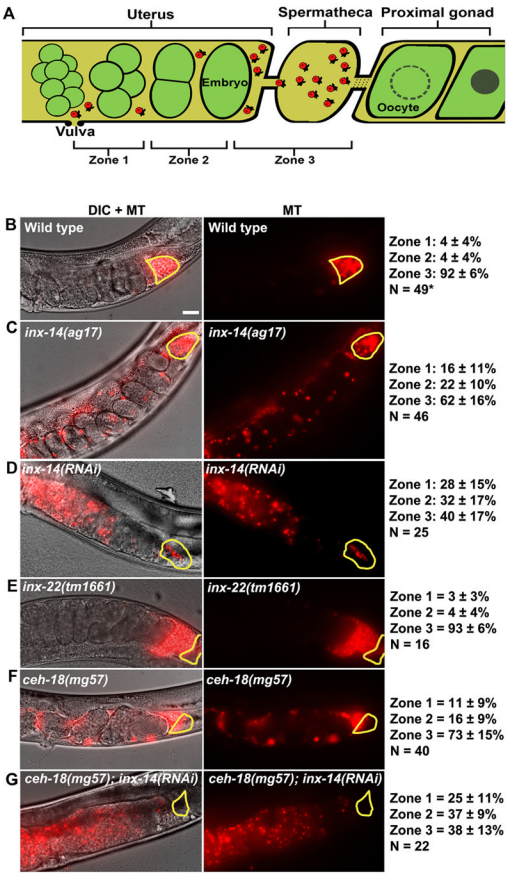

Figure 1. INX-14 acts cell nonautonomously to promote sperm guidance

(A) Sperm guidance is quantified by mating MitoTracker-labeled (MT) males to adult hermaphrodites and measuring sperm accumulation 1 hour after mating in each of the three defined zones.

(B–G) Sperm distribution within the uterus 1 hour after mating. The spermatheca is outlined in yellow. Feeding RNAi was initiated at the L4 stage. Values +/− SD are shown. *, wild type sperm accumulation values were previously published. Bar, 20 μm.

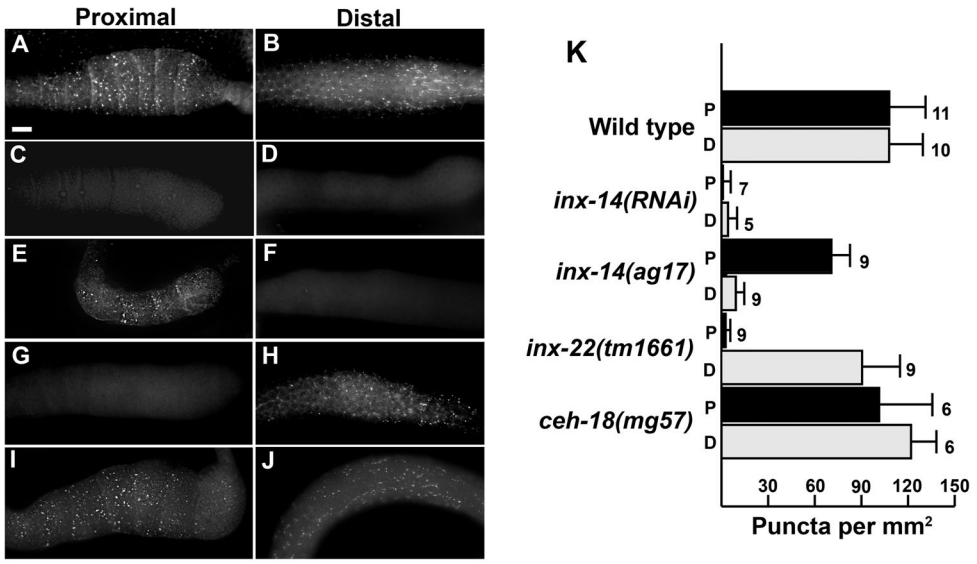

Figure 2. INX-14 localization in wild-type and mutant hermaphrodite gonads

(A–J) Immunocytochemical detection of INX-14 in wild type (A, B), *inx-14(RNAi)* (C, D), *inx-14(ag17)* (E, F), *inx-22(tm1661)* (G, H), and *ceh-18(mg57)* (I, J) proximal and distal dissected gonads. Bar, 20 μm.

(K) Quantification of INX-14 puncta per mm^2 sheath/germ cell interface surface area. Error bars are SD. The number of gonads analyzed is to the right of each bar. P, Proximal; D, Distal.

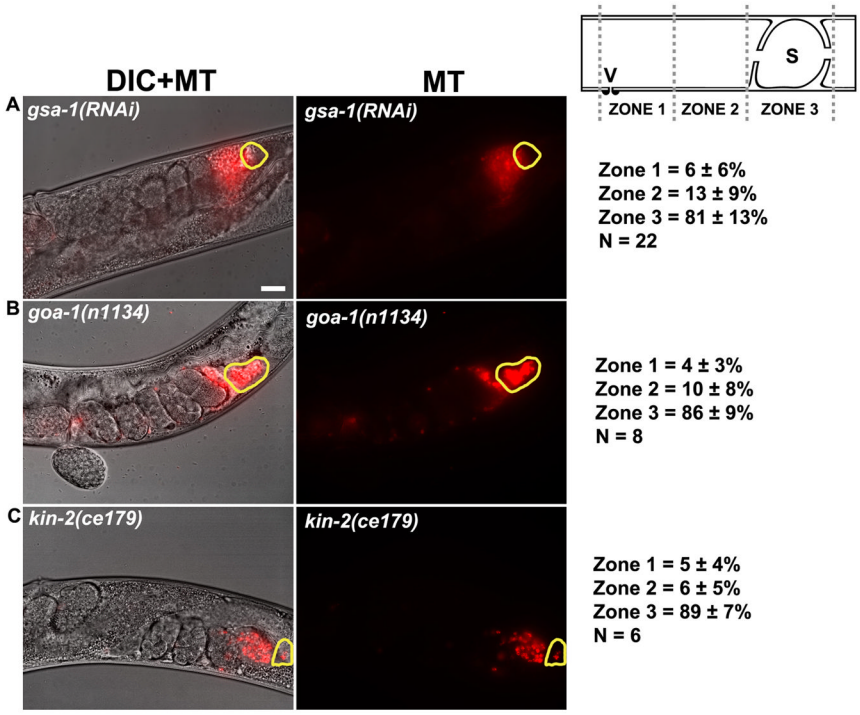

Figure 3. Genes required for proximal sheath/oocyte gap junction signal transduction are not essential for sperm guidance

Representative images and quantification of sperm accumulation in mutant and RNAi hermaphrodite uteri. *gsa-1* encodes a G_s alpha subunit of heterotrimeric G proteins, *goa-1* encodes a heterotrimeric G alpha subunit G_o, and *kin-2* encodes a regulatory subunit of a cAMP-dependent protein kinase. The spermatheca is outlined in yellow. Scale bar, 20 μm. Schematic of zone definitions is shown to the right. V, vulva; S, spermatheca; n, number of gonad arms quantified. Values +/− SD are shown.

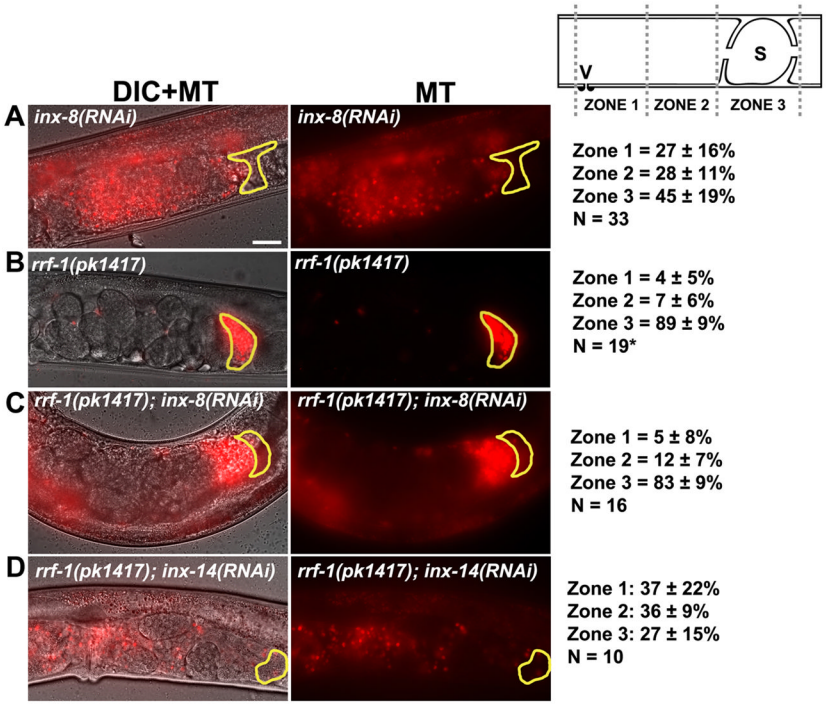

Figure 4. Site of innexin action in sperm guidance

(A–D) Representative images and quantification of sperm accumulation in mutant and RNAi hermaphrodite uteri. *rrf-1(pk1417)* are sensitive to RNAi in the germ line, but not in the somatic gonadal cells (Sijen et al., 2001). The spermatheca is outlined in yellow. Scale bar, 20 μm. Schematic of zone definitions is shown to the right of panel A. V, vulva; S, spermatheca; n, number of gonad arms quantified. Values +/− SD are shown. *, *rrf-1(pk1417)* sperm accumulation values were previously published (Edmonds et al., 2010). Intestinal autofluorescence can be seen in panels A, C, and D.

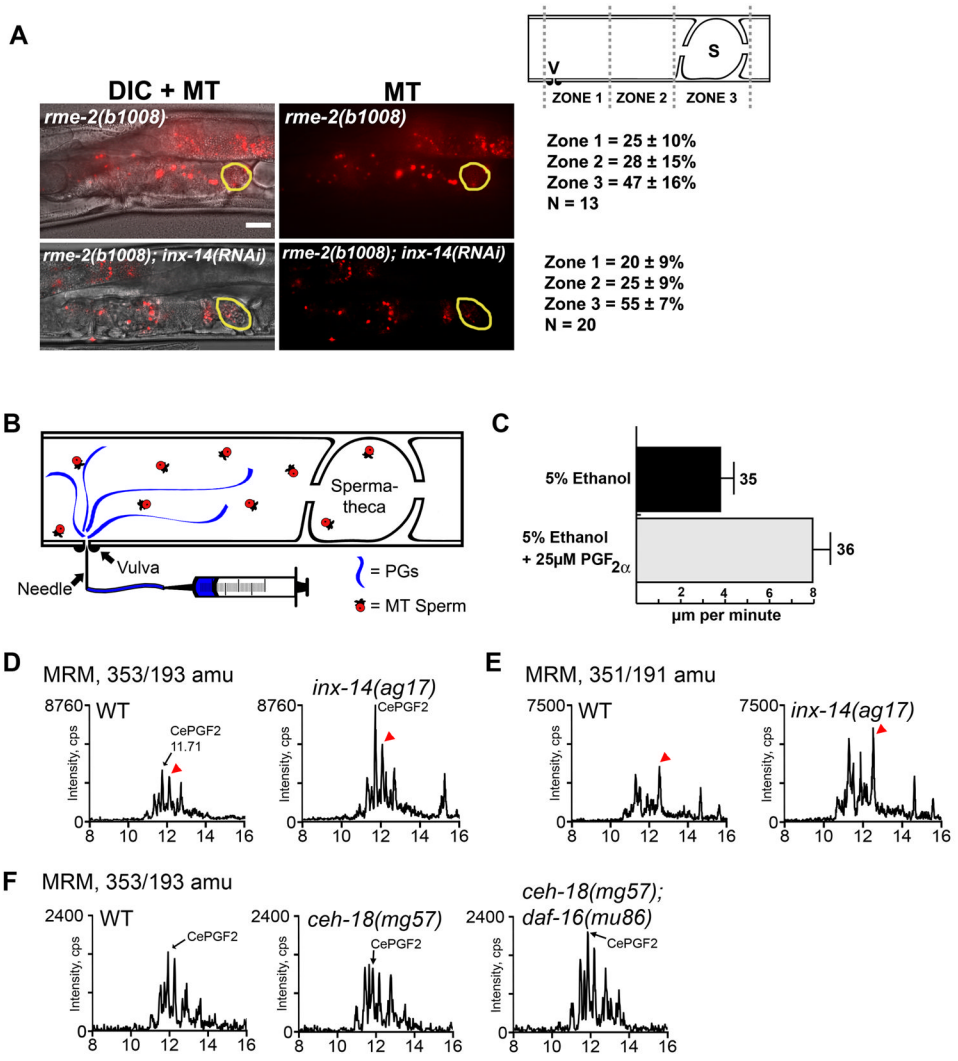

Figure 5. INX-14 acts downstream of F-series prostaglandin synthesis

(A) Representative images and quantification of sperm accumulation in mutant and RNAi hermaphrodite uteri. The spermatheca is outlined in yellow. Scale bar, 20 μm. Schematic of zone definitions is shown to the right. V, vulva; S, spermatheca; n, number of gonad arms quantified. Values +/− SD are shown. Intestinal autofluorescence can be seen in both panels.

(B) Diagram of microinjection method. Sperm velocities are quantified from time-lapse video generated approximately 5 minutes after microinjection through the vulva. $PGF_{2\alpha}$ in 5% ethanol or 5% ethanol control was injected through the vulva into the uterus of *inx-14(RNAi)* hermaphrodites after mating to wild-type MT-stained males.

(C) Sperm velocity in *inx-14(RNAi)* microinjected uteri. WT sperm migrate at 8 μm per minute in WT hermaphrodites (Kubagawa et al., 2006). Error bars are SEM. Number of sperm analyzed after microinjection is shown to the right of each bar.

(D) MRM chromatogram using the mass transition *m/z* 353/193, which detects $PGF_{2\alpha}$-like prostaglandins (Murphy et al., 2005). HPLC retention times, which are based on lipid hydrophobicity, are shown on the X-axis. CePGF2 and a structurally related prostaglandin (red arrowhead) are synthesized largely by oocytes (Edmonds et al., 2010).

(E) MRM chromatogram using the mass transition *m/z* 351/191, which detects PGF_3-like prostaglandins (Murphy et al., 2005). HPLC retention times are shown on the X-axis. Red

arrowhead indicates prostaglandin previously shown to be synthesized largely by oocytes (Edmonds et al., 2010). Whether other prostaglandins in this chromatogram are synthesized by oocytes is currently not known.

(F) MRM chromatogram using the mass transition *m/z* 353/193. HPLC retention times are shown on the X-axis. Experiments shown in panels D and E were conducted independent of those in panel F using different wild-type cultures. Similar results were observed in two independent replicates.

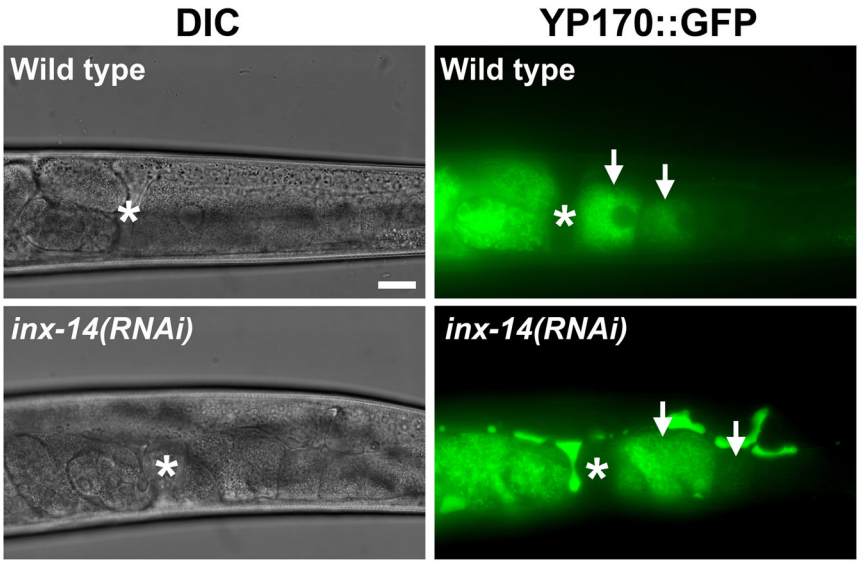

Figure 6. Yolk transport in wild-type and *inx-14(RNAi)* gonads

A vitellogenin::green fluorescent protein (YP170::GFP) fusion is used to monitor yolk lipoprotein complex localization (Grant and Hirsh, 1999). Arrows indicate oocytes. Asterisks indicate the spermatheca with fertilized embryos to the left in the uterus. Excess yolk is found in the pseudocoelom of *inx-14(RNAi)* hermaphrodites, suggesting that yolk synthesis rates are increased or endocytosis rates are reduced. Scale bar, 20 μm.

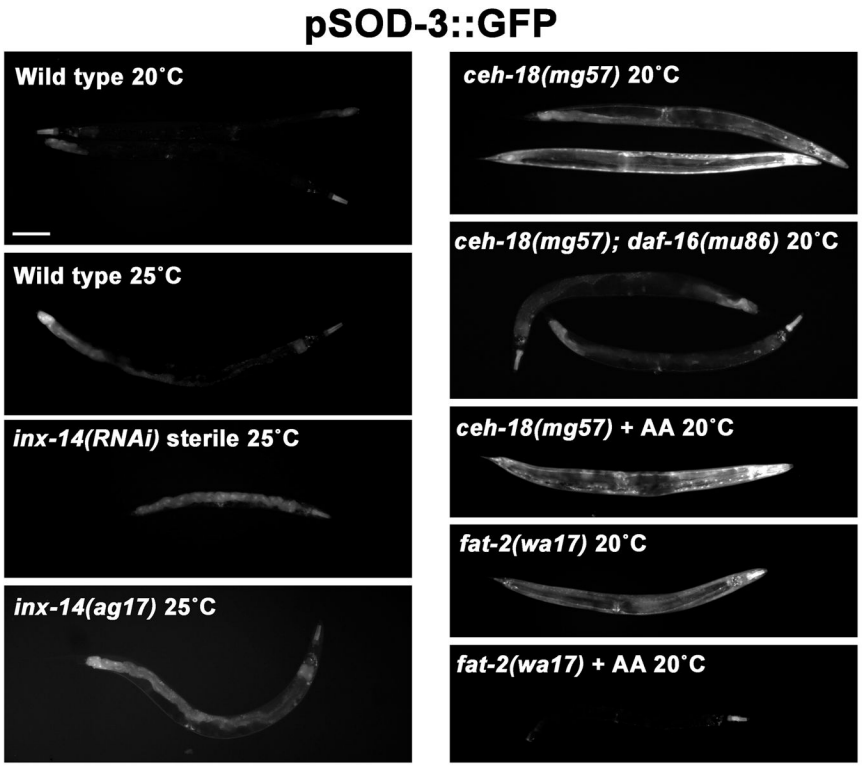

Figure 7. *inx-14* and *ceh-18* inhibit DAF-16/FOXO transcriptional activity

Integrated *sod-3p::gfp* transgene expression in wild type and mutant hermaphrodites. The *sod-3* promotes is a direct DAF-16 target and GFP expression in the intestine and other tissues is indicative of DAF-16 transcriptional activity (Henderson et al., 2006; Oh et al., 2006). Miyata et al. (2008) have shown that *inx-14(ag17)* mutants have elevated DAF-16-dependent *sod-3* expression. AA indicates arachidonic acid supplementation. Scale bar, 100 μm.

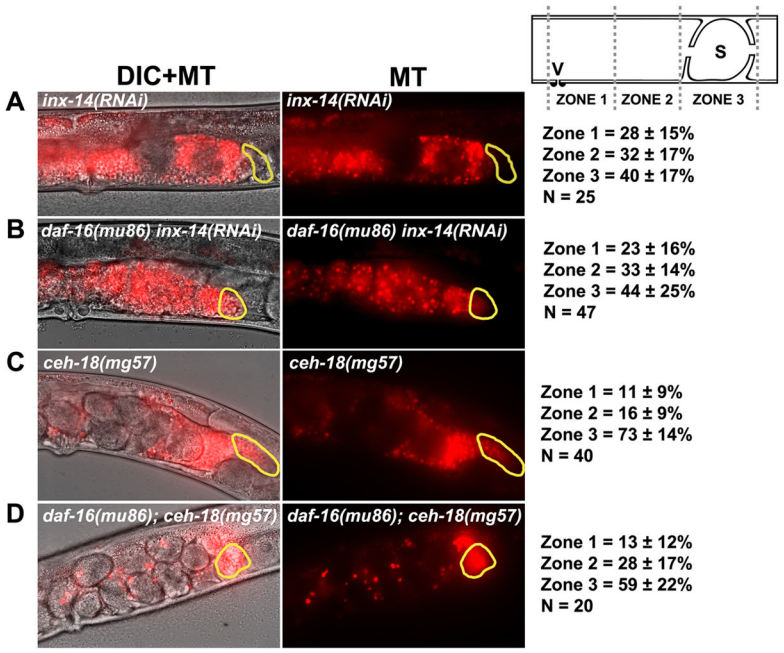

E

Genotype	Fertilized Eggs	N
inx-14(RNAi)	28.1 ± 7.8	19
daf-16(mu86) inx-14(RNAi)	44.9 ± 21.9	11
ceh-18(mg57)	188.2 ± 59.2	29
daf-16(mu86); ceh-18(mg57)	177.5 ± 53.1	53

Figure 8. *inx-14* and *ceh-18* regulate sperm guidance independent of DAF-16/FOXO

(A–D) Representative images and quantification of sperm accumulation in adult mutant hermaphrodite uteri. The spermatheca is outlined in yellow. Scale bar, 20 μm. Schematic of zone definitions is shown to the right of panel A. V, vulva; S, spermatheca; n, number of gonads quantified. Values +/− SD are shown. *daf-16(mu86)* hermaphrodites have mild sperm guidance defects, with zone 3 accumulation at 80% (N = 48). Data in panels A and C are from Figure 1. Zone 3 accumulation in *daf-16(mu86); ceh-18(mg57)* mutants is significantly less than accumulation in *ceh-18(mg57)* mutants ($P < 0.01$).

(E) Fertilized eggs laid on plates in mutant and RNAi hermaphrodites. Hermaphrodite mutants with impaired oocyte prostaglandin synthesis lose self-derived sperm due to failure to maintain spermathecal position, causing reduced fertilized egg production (Edmonds et al., 2010; Kubagawa et al., 2006). Values +/− SD are shown. N is the number of hermaphrodites scored.

Table 1

Sperm motility values in hermaphrodite uteri

Hermaphrodite Description	Avg Vel (μm/min)	Avg Vvel (μm/min)	Rev Freq (rev/hr)	N
1. WT	8.10 ± 0.52	4.76 ± 0.64	1.62 ± 0.51	102*
2. *inx-14(ag17)*	3.99 ± 0.46	0.70 ± 0.61	8.53 ± 3.38	20
3. *inx-14(RNAi)*	4.42 ± 0.29	−0.78 ± 0.36	15.84 ± 2.35	33
4. *inx-22(tm1661)*	7.93 ± 0.65	5.32 ± 0.54	4.11 ± 2.79	10
5. *ceh-18(mg57)*	6.98 ± 0.50	1.60 ± 0.85	9.19 ± 2.90	36

Sperm motility values in WT and mutant hermaphrodite uteri were measured from time-lapse videos immediately after mating to MT males. Average vectorial velocity (Avg Vvel) is directional velocity toward the spermatheca. Reversals (Rev Freq, reversal frequency) were defined as >90 degree turns in three subsequent time-lapse frames. N indicates the number of sperm analyzed.

*, WT sperm values include new data (N=10) and published data (Edmonds et al., 2010). Values +/− SEM are shown.